

Gesture-Aware Pretraining and Token Fusion for 3D Hand Pose Estimation

Rui Hong, Jana Kořecká
George Mason University
{rhong5, kosecka}@gmu.edu

Abstract

Estimating 3D hand pose from monocular RGB images is fundamental for applications in AR/VR, human–computer interaction, and sign language understanding. In this work we focus on a scenario where a discrete set of gesture labels is available and show that gesture semantics can serve as a powerful inductive bias for 3D pose estimation. We present a two-stage framework: gesture-aware pretraining that learns an informative embedding space using coarse and fine gesture labels from InterHand2.6M [12], followed by a per-joint token Transformer guided by gesture embeddings as intermediate representations for final regression of MANO hand parameters [16]. Training is driven by a layered objective over parameters, joints, and structural constraints. Experiments on InterHand2.6M demonstrate that gesture-aware pretraining consistently improves single-hand accuracy over the state-of-the-art EANet [13] baseline, and that the benefit transfers across architectures without any modification.

1. Introduction

Estimating 3D hand pose from monocular RGB images is a fundamental problem with broad applications in augmented/virtual reality, human–computer interaction, robotics, and sign language recognition. Despite rapid progress, the task remains challenging due to severe self-occlusions, large articulation ranges, foreshortening, and depth ambiguity.

Most existing approaches build upon the MANO parametric model [16] and regress hand pose and shape parameters from an RGB image, varying in their intermediate representations, architectures, and learning strategies. Early works, inspired by the success of SMPL for human mesh recovery [8], directly regressed MANO parameters from images [1, 2, 17, 24]. Follow-up methods improved performance using 2D keypoint heatmaps or larger-scale datasets [4, 5, 25]. Structural constraints—bone length

consistency, bone continuity, interpenetration penalties—improved anatomical plausibility but do not address semantic variation [2, 21, 24]. These advances exploit mostly geometric constraints and operate in a general setting, rarely leveraging the *semantic regularities* of hand gestures. In many application domains, such as sign language, hand shapes correspond to lexical units and exhibit recurring sub-configurations (e.g., characteristic finger closures) that constrain feasible poses and aid disambiguation under occlusion or low texture. Embedding such priors in the visual encoder can guide feature formation and stabilize downstream structured reasoning.

Overview of our approach. We introduce a two-stage approach coupling gesture-aware pretraining with gesture-guided fusion for robust 3D hand pose estimation. In Stage 1, we pretrain an HRNet [20] on InterHand2.6M single-hand images with hierarchical gesture classification (coarse and fine labels), endowing the encoder with semantics-sensitive features. In Stage 2, the model computes per-joint tokens by integrating global image features with a 2.5D volumetric representation and refines them via a Transformer guided by gesture embeddings as intermediate representations to predict 3D hand pose. Our contributions are:

- A **gesture-aware pretraining** strategy that equips a high-resolution encoder with coarse-to-fine gesture semantics, motivated by the connection between hand pose and linguistic meaning in sign language [7].
- A **gesture-guided fusion framework** that uses gesture embeddings as intermediate representations to guide per-joint token refinement via a Transformer.
- Experimental validation showing that the proposed pretraining **transfers across architectures**: plugging our gesture-pretrained backbone into EANet [13] without any other modification consistently reduces error on InterHand2.6M.

2. Related Work

Single-Hand 3D Pose Estimation. Early approaches employed the MANO hand model [16] and directly regressed pose and shape parameters from an image [1, 2, 17, 24], achieving compactness but struggling under occlusion. Volumetric and 2.5D intermediate representations [4, 5, 25] provided stronger spatial supervision. HaMeR [14] and WiLoR [15] further improved robustness in challenging in-the-wild settings by pretraining on large mixed datasets including InterHand2.6M, followed by fine-tuning on target benchmarks such as FreiHand [25].

Two-Hand Interactions. InterHand2.6M [12] provided the first large-scale two-hand dataset. Subsequent methods address the resulting severe mutual occlusion and co-articulation via cross-hand attention [11], attentive implicit fields [10], extract-and-adapt strategies [13], and part-based attention [22]. Our work focuses on single-hand estimation; extending gesture semantics to two-hand scenarios is a promising direction for future work.

Gesture Semantics. Gesture-aware representations have been exploited for sign language recognition [3, 6, 7, 9], but have not been utilized for 3D hand pose estimation. Our work bridges this gap by explicitly integrating gesture-aware pretraining into a pose estimation pipeline.

3. Methodology

The proposed approach consists of two stages: (1) gesture-aware pretraining of an HRNet encoder with coarse- and fine-grained gesture supervision, and (2) per-joint tokenization and gesture-guided fusion for 3D pose estimation. We adopt HRNet [20] as the backbone, using its feature levels F_4 and F_5 as multi-scale representations.

3.1. Stage 1: Gesture-Aware Pretraining

HRNet maintains high-resolution feature maps throughout the network by connecting multi-resolution branches in parallel and repeatedly exchanging information across them—a design proven effective for dense prediction tasks including human pose estimation [18], hand pose estimation [15], object detection [20], and semantic segmentation [19]. We extend HRNet to hand pose estimation and equip it with gesture-aware pretraining to inject semantic priors.

Among HRNet’s feature levels, F_4 preserves higher-resolution spatial detail while F_5 captures more semantic representations. The global feature vector $\mathbf{g} \in \mathbb{R}^{512}$ is the pooled output of $F_5 \in \mathbb{R}^{512 \times 16 \times 16}$:

$$\mathbf{g} = \text{Flatten}(\text{Pool}(F_5)).$$

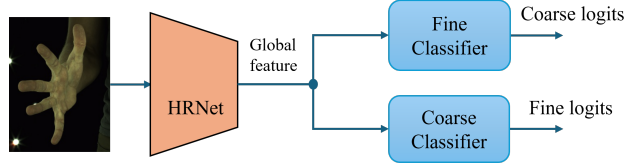


Figure 1. Stage 1: gesture-aware pretraining. HRNet global features \mathbf{g} feed two classification heads. A gradual weighting schedule stabilizes coarse categories first before incorporating fine distinctions.

Table 1. Example gesture labeling. $c_i \in [0, 54)$: coarse index; $f_j \in [0, 70)$: fine index.

| Image | Coarse (c_i) | Fine (f_j) |
|--------------|------------------|----------------|
| Top-left | c_1 | f_1 |
| Top-right | c_1 | f_1 |
| Bottom-left | c_2 | f_2 |
| Bottom-right | c_2 | f_3 |

Two lightweight classification heads predict gesture logits from \mathbf{g} :

$$\gamma_{\text{coarse}} = f_{\text{coarse}}(\mathbf{g}), \quad \gamma_{\text{fine}} = f_{\text{fine}}(\mathbf{g}),$$

and are trained with cross-entropy under a combined objective:

$$L_{\text{cls}} = L_{\text{coarse}} + \alpha L_{\text{fine}}.$$

To stabilize training, α is gradually increased from 0.1 by 0.12 every 10 epochs up to a maximum of 0.5, prioritizing coarse semantic separation early and progressively incorporating fine-grained cues. An overview of Stage 1 is shown in Fig. 1.

After pretraining, the encoder produces multi-scale features $\{F_4, F_5\}$, global feature \mathbf{g} , and gesture logits $(\gamma_{\text{coarse}}, \gamma_{\text{fine}})$ reused in Stage 2.

Gesture label construction. InterHand2.6M contains 90 folders of single-hand gesture sequences. We manually inspected images across folders and merged visually indistinguishable gestures into a shared label, while assigning subtle variants to distinct *fine* labels under a common *coarse* category. This yielded 54 coarse and 70 fine gesture categories used as Stage 1 supervision.

As shown in Fig. 2, folders “0038_fingerspreadnormal” and “0027_five_count” are visually identical and receive the same label at both levels. Conversely, “0007_thumbup_normal” and “0006_thumbup_relaxed” share a coarse label but differ in fine label due to a subtle thumb position difference (Tab. 1).

3.2. Stage 2: Gesture-Guided 3D Pose Estimation

Stage 2 constructs per-joint tokens from HRNet multi-scale features using a 2.5D volumetric representation, then refines

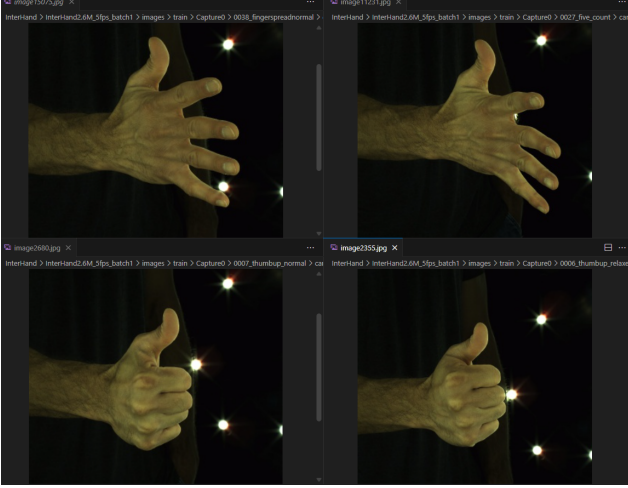


Figure 2. Example gesture images. Top: “fingerspreadnormal” and “five_count” (same label). Bottom: “thumbup_normal” and “thumbup_relaxed” (same coarse, different fine label).

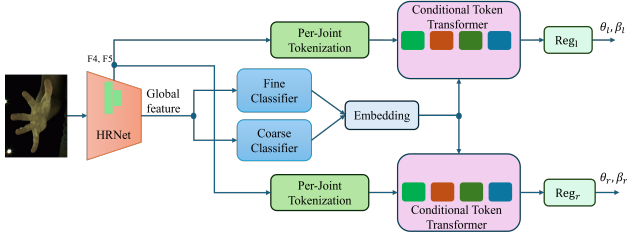


Figure 3. Stage 2 pipeline. Multi-scale features (F_4, F_5) feed the per-joint tokenization module. Stage 1 gesture logits ($\gamma_{\text{coarse}}, \gamma_{\text{fine}}$) are embedded and injected into the gesture-guided Transformer. Outputs are decoded to MANO parameters (θ, β).

them via a Transformer guided by Stage 1 gesture embeddings as intermediate representations. The full pipeline is shown in Fig. 3.

From the pretrained HRNet encoder we take $F_4 \in \mathbb{R}^{256 \times 32 \times 32}$ and $F_5 \in \mathbb{R}^{512 \times 16 \times 16}$, and the global descriptor $\mathbf{g} \in \mathbb{R}^{512}$. The Stage 1 gesture logits ($\gamma_{\text{coarse}}, \gamma_{\text{fine}}$) are projected into the token embedding space via two independent two-layer MLPs:

$$\mathbf{e}_{\text{coarse}} = \phi_{\text{coarse}}(\gamma_{\text{coarse}}), \quad \mathbf{e}_{\text{fine}} = \phi_{\text{fine}}(\gamma_{\text{fine}}),$$

$$\mathbf{e}_{\text{coarse}}, \mathbf{e}_{\text{fine}} \in \mathbb{R}^{1024}.$$

Per-Joint Tokenization via 2.5D Volumetric Reasoning F_4 and F_5 are each projected to $\mathbb{R}^{512 \times 16 \times 16}$ and concatenated along channels to form $\mathbf{F} \in \mathbb{R}^{1024 \times 16 \times 16}$. Flattening yields a global token sequence $\mathbf{T} \in \mathbb{R}^{256 \times 1024}$, which is passed through a lightweight Transformer encoder and reshaped to a spatial feature map $\mathbf{F}' \in \mathbb{R}^{1024 \times 16 \times 16}$.

A volumetric head predicts a full 3D heatmap volume per joint, $\mathbf{H} \in \mathbb{R}^{J \times 16 \times 16 \times 16}$, $J=21$. Joint locations are estimated via soft-argmax over this volume:

$$(\hat{x}, \hat{y}, \hat{z}) = \sum_{x,y,z} (x, y, z) \frac{\exp(\mathbf{H}(j, x, y, z))}{\sum_{x',y',z'} \exp(\mathbf{H}(j, x', y', z'))},$$

where (\hat{x}, \hat{y}) lie in the image plane and \hat{z} is a wrist-relative depth offset rather than metric depth. We refer to this as a 2.5D representation following [12]: the volume itself is 3D, but the z -axis encodes relative depth rather than absolute 3D position, distinguishing it from full metric 3D reconstruction. Using (\hat{x}, \hat{y}) , we sample \mathbf{F}' via `grid.sample` to obtain per-joint tokens $\mathbf{U} \in \mathbb{R}^{1024 \times J}$.

Transformer Module with Gesture Guidance Tokens

The per-joint tokens are linearly projected and augmented with a learnable positional encoding:

$$\mathbf{Q} = \mathbf{U}^\top \mathbf{W} + \mathbf{E}_{\text{pos}}, \quad \mathbf{Q} \in \mathbb{R}^{J \times 1024}.$$

Gesture guidance tokens are formed as:

$$\mathbf{c}_* = \sigma(s_*) (\mathbf{e}_* + \mathbf{t}_*), \quad * \in \{\text{coarse}, \text{fine}\},$$

where \mathbf{t}_* is a learnable type embedding and s_* is a scalar gate initialized near zero for stable training. The joint and gesture guidance tokens are concatenated:

$$\mathbf{S} = [\mathbf{Q}; \mathbf{c}_{\text{coarse}}; \mathbf{c}_{\text{fine}}] \in \mathbb{R}^{(J+2) \times 1024},$$

and processed by a Transformer encoder, retaining only the first J positions:

$$\mathbf{O} = (\mathcal{E}(\mathbf{S}))_{1:J} \in \mathbb{R}^{J \times 1024}.$$

A residual connection fuses refined tokens back with the original per-joint features:

$$\tilde{\mathbf{U}} = \mathbf{U} + \text{Post}(\mathbf{O}^\top), \quad \tilde{\mathbf{U}} \in \mathbb{R}^{1024 \times J},$$

where `Post(\cdot)` is a learnable 1×1 convolution.

MANO Parameter Regression From $\tilde{\mathbf{U}}$, two MLP heads regress MANO parameters: (i) a pose head predicting joint rotations in the 6D representation [23] for continuity and stability, and (ii) a shape head regressing shape coefficients $\beta \in \mathbb{R}^{10}$.

Training Objective The training loss combines three levels of supervision:

$$\begin{aligned} \mathcal{L} = & \lambda_p L_{\text{pose}} + \lambda_s L_{\text{shape}} \\ & + \lambda_{3D} L_{3D} + \lambda_{\text{mano-3D}} L_{\text{mano-3D}} + \lambda_{2.5D} L_{2.5D} \\ & + \lambda_{2D} L_{2D} + \lambda_{\text{mano-2D}} L_{\text{mano-2D}} \\ & + \lambda_{\text{cont}} L_{\text{cont}}, \end{aligned} \quad (1)$$

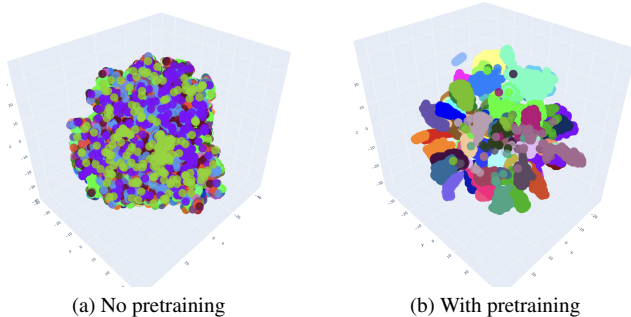


Figure 4. t-SNE of HRNet pooled features on InterHand2.6M test set, colored by coarse gesture label. Gesture pretraining yields more discriminative representations.

with weights $\lambda_p=2$, $\lambda_s=0.5$, $\lambda_{3D}=\lambda_{\text{mano-3D}}=20$, $\lambda_{2D}=\lambda_{\text{mano-2D}}=0.5$, $\lambda_{2.5D}=0.05$, $\lambda_{\text{cont}}=10$.

Parameter-level. L_{pose} and L_{shape} are ℓ_1 losses on the predicted MANO pose parameters (6D joint rotations) and shape coefficients β , respectively.

Joint-level. L_{3D} is an ℓ_1 loss on camera-space 3D joint positions obtained from the 2.5D soft-argmax predictions. $L_{\text{mano-3D}}$ is an ℓ_1 loss on the 3D joints produced by the MANO forward kinematics layer from the regressed parameters. $L_{2.5D}$ is an ℓ_1 loss on the 2.5D heatmap coordinates (image-plane location and wrist-relative depth) predicted by the volumetric head. L_{2D} and $L_{\text{mano-2D}}$ are the corresponding 2D reprojection losses for the soft-argmax and MANO joints, respectively.

Structural. L_{cont} enforces bone continuity along kinematic chains by penalizing discontinuities in consecutive joint rotations, encouraging anatomically smooth poses.

4. Experiments

We evaluate on the single-hand subset of InterHand2.6M [12] and report MPJPE and MPVPE in millimeters. All methods in Tab. 2 are trained on single-hand images of InterHand2.6M, except HaMeR which is pretrained on a large mixed dataset without InterHand2.6M fine-tuning; its higher error reflects this domain gap rather than a fundamental limitation of the approach.

4.1. Gesture-Aware Pretraining Analysis

We analyze the effect of gesture pretraining via t-SNE on the test set. As shown in Fig. 4, baseline HRNet features exhibit poor inter-class separation, while pretrained features form clearer clusters, suggesting improved encoder discriminability. Fig. 5 shows that the coarse and fine classifier outputs exhibit different cluster granularities, consistent with the intended coarse-to-fine supervision hierarchy.

4.2. Single-Hand 3D Pose Estimation

Results are shown in Tab. 2.

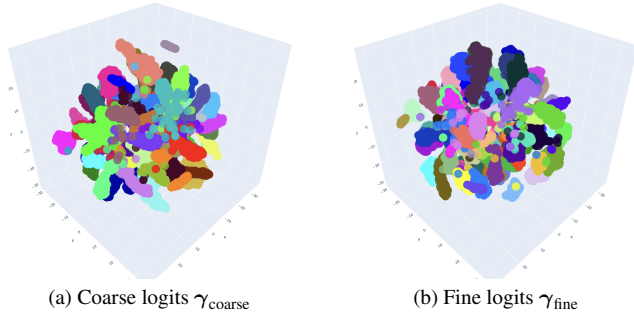


Figure 5. t-SNE of classifier outputs on InterHand2.6M test set. Coarse and fine logits exhibit different cluster granularities, consistent with the coarse-to-fine supervision design.

Table 2. Single-hand results on InterHand2.6M test set (mm). PT denotes gesture-aware pretraining; full model additionally injects gesture guidance tokens in Stage 2.

| Method | MPJPE ↓ | MPVPE ↓ |
|--------------------------------|-------------|-------------|
| HaMeR [14] | 16.11 | 15.37 |
| EANet [13] | 4.94 | 5.26 |
| EANet (w/ gesture pretraining) | 4.86 | 5.17 |
| Ours (w/o PT) | 5.00 | 5.35 |
| Ours (full) | 4.84 | 5.19 |

Effect on our method. Adding gesture pretraining and gesture guidance reduces both MPJPE and MPVPE, showing that gesture priors improve both feature learning in Stage 1 and token refinement in Stage 2.

Cross-architecture transferability. Replacing EANet’s ImageNet-pretrained ResNet-50 with our gesture-pretrained backbone—with no other changes to EANet—consistently reduces error. This suggests that the benefit of gesture-aware pretraining is architecture-agnostic, making it a general-purpose component for single-hand pose estimation.

Qualitative results. Fig. 6 compares EANet and our full method under occlusion. In both examples, EANet produces mesh interpenetration artifacts (red ellipses), while our method yields more anatomically plausible meshes, suggesting that gesture-aware features help resolve ambiguous occluded poses.

5. Conclusion

We presented a gesture-aware pretraining strategy and a gesture-guided token fusion framework for single-hand 3D pose estimation. The key finding is that gesture semantics—learned from coarse-to-fine hierarchical supervision on

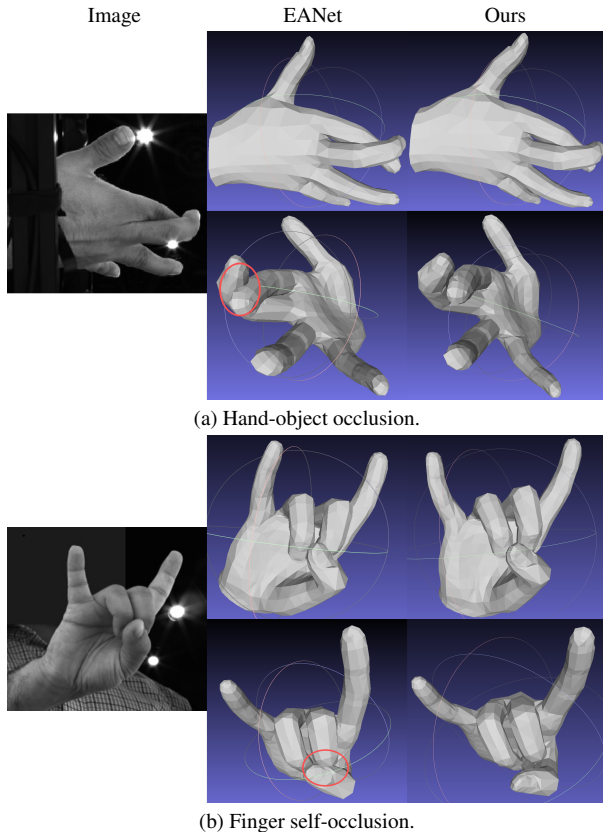


Figure 6. Qualitative comparison under occlusion. Our method produces more plausible hand meshes without interpenetration artifacts.

single-hand images—provide a useful and transferable inductive bias: they improve accuracy in our own architecture and transfer directly to EANet without any modification, suggesting their general utility. Our method also produces more anatomically plausible meshes under occlusion, attributed to the semantic constraints imposed by gesture pretraining. Extending gesture-aware pretraining to two-hand and in-the-wild settings remains a promising direction for future work.

References

- [1] Adnane Boukhayma, Rodrigo de Bem, and Philip HS Torr. 3d hand shape and pose from images in the wild. In *Proceedings of the IEEE/CVF conference on computer vision and pattern recognition*, pages 10843–10852, 2019. 1, 2
- [2] Yujun Cai, Lihao Ge, Jianfei Cai, and Junsong Yuan. Weakly-supervised 3d hand pose estimation from monocular rgb images. In *Proceedings of the European conference on computer vision (ECCV)*, pages 666–682, 2018. 1, 2
- [3] Necati Cihan Camgoz, Simon Hadfield, Oscar Koller, and Richard Bowden. Subunets: End-to-end hand shape and continuous sign language recognition. In *Proceedings of the IEEE International Conference on Computer Vision (ICCV)*, pages 22–27, 2017. 2
- [4] Yujin Chen, Zhigang Tu, Di Kang, Linchao Bao, Ying Zhang, Xuefei Zhe, Ruizhi Chen, and Junsong Yuan. Model-based 3d hand reconstruction via self-supervised learning. In *Proceedings of the IEEE/CVF conference on computer vision and pattern recognition*, pages 10451–10460, 2021. 1, 2
- [5] Lihao Ge, Zhou Ren, Yuncheng Li, Zehao Xue, Yingying Wang, Jianfei Cai, and Junsong Yuan. 3d hand shape and pose estimation from a single rgb image. In *Proceedings of the IEEE/CVF conference on computer vision and pattern recognition*, pages 10833–10842, 2019. 1, 2
- [6] Shester Gueuwou, Xiaodan Du, Greg Shakhnarovich, Karen Livescu, and Alexander H. Liu. SHuBERT: Self-supervised sign language representation learning via multi-stream cluster prediction. In *Proceedings of the 63rd Annual Meeting of the Association for Computational Linguistics (Volume 1: Long Papers)*, pages 28792–28810, Vienna, Austria, 2025. Association for Computational Linguistics. 2
- [7] Al Amin Hosain, Panneer Selvam Santhalingam, Parth Pathak, Huzefa Rangwala, and Jana Kosecka. FineHand: Learning hand shapes for american sign language recognition, 2020. 1, 2
- [8] Angjoo Kanazawa, Michael J. Black, David W. Jacobs, and Jitendra Malik. End-to-end recovery of human shape and pose. In *Proceedings of the IEEE Conference on Computer Vision and Pattern Recognition (CVPR)*, pages 7122–7131, 2018. 1
- [9] Oscar Koller, Hermann Ney, and Richard Bowden. Deep hand: How to train a cnn on 1 million hand images when your data is continuous and weakly labelled. In *Proceedings of the IEEE Conference on Computer Vision and Pattern Recognition (CVPR)*, pages 3793–3802, Las Vegas, NV, USA, 2016. 2
- [10] Jihyun Lee, Minhyuk Sung, Honggyu Choi, and Tae-Kyun Kim. Im2hands: Learning attentive implicit representation of interacting two-hand shapes. In *Proceedings of the IEEE/CVF conference on computer vision and pattern recognition*, pages 21169–21178, 2023. 2
- [11] Mengcheng Li, Liang An, Hongwen Zhang, Lianpeng Wu, Feng Chen, Tao Yu, and Yebin Liu. Interacting attention graph for single image two-hand reconstruction. In *Proceedings of the IEEE/CVF conference on computer vision and pattern recognition*, pages 2761–2770, 2022. 2
- [12] Gyeongsik Moon, Shoou-I Yu, He Wen, Takaaki Shiratori, and Kyoung Mu Lee. Interhand2. 6m: A dataset and baseline for 3d interacting hand pose estimation from a single rgb image. In *European Conference on Computer Vision*, pages 548–564. Springer, 2020. 1, 2, 3, 4
- [13] JoonKyu Park, Daniel Sungho Jung, Gyeongsik Moon, and Kyoung Mu Lee. Extract-and-adaptation network for 3d interacting hand mesh recovery. In *Proceedings of the IEEE/CVF International Conference on Computer Vision*, pages 4200–4209, 2023. 1, 2, 4
- [14] Georgios Pavlakos, Dandan Shan, Ilija Radosavovic, Angjoo Kanazawa, David Fouhey, and Jitendra Malik. Reconstructing hands in 3d with transformers. In *Proceedings of*

- the IEEE/CVF Conference on Computer Vision and Pattern Recognition*, pages 9826–9836, 2024. 2, 4
- [15] Rolandos Alexandros Potamias, Jinglei Zhang, Jiankang Deng, and Stefanos Zafeiriou. Wilor: End-to-end 3d hand localization and reconstruction in-the-wild. In *Proceedings of the Computer Vision and Pattern Recognition Conference*, pages 12242–12254, 2025. 2
- [16] Javier Romero, Dimitrios Tzionas, and Michael J Black. Embodied hands: Modeling and capturing hands and bodies together. In *ACM Transactions on Graphics (TOG)*, 2017. 1, 2
- [17] Yu Rong, Takaaki Shiratori, and Hanbyul Joo. Frankmocap: A monocular 3d whole-body pose estimation system via regression and integration. In *Proceedings of the IEEE/CVF International Conference on Computer Vision Workshops (ICCV Workshops)*, pages 1749–1759, 2021. 1, 2
- [18] Ke Sun, Bin Xiao, Dong Liu, and Jingdong Wang. Deep high-resolution representation learning for human pose estimation. In *Proceedings of the IEEE/CVF conference on computer vision and pattern recognition*, pages 5693–5703, 2019. 2
- [19] Ke Sun, Yang Zhao, Borui Jiang, Tianheng Cheng, Bin Xiao, Dong Liu, Yadong Mu, Xinggang Wang, Wenyu Liu, and Jingdong Wang. High-resolution representations for labeling pixels and regions. *arXiv preprint arXiv:1904.04514*, 2019. 2
- [20] Jingdong Wang, Ke Sun, Tianheng Cheng, Borui Jiang, Chaorui Deng, Yang Zhao, Dong Liu, Yadong Mu, Mingkui Tan, Xinggang Wang, et al. Deep high-resolution representation learning for visual recognition. *IEEE transactions on pattern analysis and machine intelligence*, 43(10):3349–3364, 2020. 1, 2
- [21] Lixin Yang, Jiasen Li, Wenqiang Xu, Yiqun Diao, and Cewu Lu. Bihand: Recovering hand mesh with multi-stage bisected hourglass networks. *arXiv preprint arXiv:2008.05079*, 2020. 1
- [22] Zhengdi Yu, Shaoli Huang, Chen Fang, Toby P Breckon, and Jue Wang. Acr: Attention collaboration-based regressor for arbitrary two-hand reconstruction. In *Proceedings of the IEEE/CVF conference on computer vision and pattern recognition*, pages 12955–12964, 2023. 2
- [23] Yi Zhou, Connelly Barnes, Jingwan Lu, Jimei Yang, and Hao Li. On the continuity of rotation representations in neural networks. In *Proceedings of the IEEE/CVF conference on computer vision and pattern recognition*, pages 5745–5753, 2019. 3
- [24] Yuxiao Zhou, Marc Habermann, Weipeng Xu, Ikhsanul Habibie, Christian Theobalt, and Feng Xu. Monocular real-time hand shape and motion capture using multi-modal data. In *CVPR*, 2020. 1, 2
- [25] Christian Zimmermann, Duygu Ceylan, Jimei Yang, Bryan Russell, Max Argus, and Thomas Brox. Freihand: A dataset for markerless capture of hand pose and shape from single rgb images. In *Proceedings of the IEEE/CVF international conference on computer vision*, pages 813–822, 2019. 1, 2